



## Response Surface Methodology (RSM) Approach for Optimizing the Actuator Nozzle Design of Pressurized Metered-Dose Inhaler (pMDI)

Muhammad Faqhrurrazi Abd Rahman<sup>1,\*</sup>, Suzairin MD Seri<sup>1</sup>, Nor Zelawati Asmuin<sup>2,\*</sup>, Ishkriyat Taib<sup>1</sup>, Nur Syakirah Rabiha Rosman<sup>3</sup>

- <sup>1</sup> Department of Mechanical Engineering, Faculty of Mechanical and Manufacturing Engineering, Universiti Tun Hussein Onn, 86400 Parit Raja, Johor, Malaysia  
<sup>2</sup> Department of Aeronautical Engineering, Faculty of Mechanical and Manufacturing Engineering, Universiti Tun Hussein Onn, 86400 Parit Raja, Johor, Malaysia  
<sup>3</sup> Cell Signaling and Biotechnology Research Group (CeSBTech), Faculty of Science and Marine Environment, Universiti Malaysia Terengganu, 21030 Kuala Nerus, Terengganu, Malaysia

### ARTICLE INFO

#### Article history:

Received 1 May 2021  
 Received in revised form 15 June 2021  
 Accepted 25 June 2021  
 Available online 30 July 2021

#### Keywords:

Pressurized metered-dose inhaler; simulation; optimization; RSM; actuator nozzle

### ABSTRACT

Recently, a remarkable scientific interest in the inhalation therapy for respiratory disease was spiked attributed to the growing prevalence of asthma, chronic obstructive pulmonary disease (COPD), and coronavirus disease 2019 (COVID-19) pandemic. A pressurized metered-dose inhaler (pMDI) is the best option by providing fast and efficient symptomatic relief within the lung. However, the rapid development of new inhalation devices could be critical in this competitive environment, and optimizing the inhalation devices could be costly and time-consuming. Therefore, the computational fluid dynamic (CFD) approach was used to shorten the development time. In this study, response surface methodology (RSM) in ANSYS version 19.2 was introduced to discover the optimal design for the actuator nozzle to increase the performance of pMDI. Three (3) parameters (orifice diameter, length, and actuator angle) were optimized, and the best design was selected according to the analysis of particle tracking. The analysis of spray plume was also conducted and compared to analyze the spray plume characteristic produced by three designs. The result showed that RSM generated three (3) models for the new design of the actuator nozzle (Design A, Design B, and Design C). Among three (3) designs, actuator nozzle design C showed the highest injection particle number (232457) and the only one that produced maximum particles velocity magnitude in the acceptable ranges (35.67m/s). All three designs showed a similar pattern as maximum particle velocity magnitude decreased along the axial length until they match the air velocity (0.03-0.04 m/s). Furthermore, the spray plume length, angle, and width were observed to increase linearly with the decreasing maximum particle velocity magnitude. Thus, this study suggested that design C might have the potential as a new actuator nozzle to develop future pMDI to relieve the respiratory condition.

\* Corresponding author.

E-mail address: [hd170038@siswa.uthm.edu.my](mailto:hd170038@siswa.uthm.edu.my) (Muhammad Faqhrurrazi Abd Rahman)

\* Corresponding author.

E-mail address: [norzela@uthm.edu.my](mailto:norzela@uthm.edu.my) (Nor Zelawati Asmuin)

<https://doi.org/10.37934/cfdl.13.7.2744>

## 1. Introduction

In treating respiratory diseases, drug delivery to the lung has emerged as a crucial process [1]. Dry powder inhalers (DPIs) and pressurized metered-dose inhalers (pMDIs) are the most popular devices used among end-users. These devices can produce small drug particles which can be inhaled orally [2]. Due to their ease of use and cost-effectiveness, DPIs and pMDIs are among the most popular ways to deliver pharmaceutical drugs [3]. Active pharmaceutical ingredient (API) in DPIs has an aerodynamic size of around 1-5  $\mu\text{m}$ , suitable for inhalation [4]. However, the main issue with DPIs is that their high surface free energy is causing them to bind together via cohesive forces. As a result, they have poor flow and aerosolization efficiency and tend to stay inside the inhaler [5]. Moreover, the patient must inhale more powerfully with a DPI than with a pMDI. Poor coordination such as blowing and exhaling directly into the device can cause scattering of medicine before it can be inhaled.

Different from DPIs, pMDIs have a canister that can help to deliver the medication to the lung. Thus, pMDI is more suitable for the elderly, kids, first-time users, or people with nerve or muscle weakness. As mentioned by Yazdani *et al.*, [6] pMDI is also lowering the drug deposition in the pharynx, consequently increasing the drug deposition in the lower respiratory. The reason is that pMDI contained hydrofluoroalkane (HFA) as inhaler propellant, replacing harmful chlorofluorocarbon (CFC). HFA can produce a much smaller particle size and delivering more than 10-15% of drugs to the lower respiratory [7,8]. HFA propellants are not only non-ozone-depleting but also environmentally friendly. These advancements explained why pMDIs propelled extraordinary interest in delivering the drugs to the lung [9].

The world has witnessed tremendous growth in inhalation device applications over the past few decades. Such expansions in inhaler research and development (R&D) would help those who suffer from respiratory problems. The pMDI inhaler grew from 440 million units to 800 million units in 2000, making for more than 80% of all medical therapy devices sold globally in 2008 [10]. In 2014, there has been unprecedented growth in the inhaler market, which increased to \$36 billion, with over 90 billion inhaled doses prescribed to patients in a single year [11]. The steady growth can be attributed to the growing prevalence of asthma and chronic obstructive pulmonary disease (COPD). Furthermore, people are now experiencing the most dangerous situation regarding the novel severe acute respiratory syndrome called coronavirus 2 (SARS-CoV-2), which is the reason for the Coronavirus disease 2019 (COVID-19) pandemic [12]. The increased number of patients suffering from COVID-19 is anticipated to increase the demand for inhalers as a palliative treatment.

The development and optimization of inhalation devices experimentally will be very expensive and time-consuming. In a very competitive environment, the rapid development of new devices can be critical for their thriving market penetration. This drawback can be resolved using computational models by decreasing the number of experiments and trials. Computational fluid dynamic (CFD) models can substantially shorten the development time for a new inhalation product [13]. Several studies described the use of computational tools for specific pMDI devices using CFD and discrete phase models (or DPM) [14].

The geometry of the actuator nozzle inside pMDI is speculated to increase the performance of the pMDI [15]. The orifice diameter, length, and actuator angle might significantly affect the formulation's atomization. To increase the drug deposition in the lower respiratory, the design of the pMDI actuator is a critical subsystem that directly impacts the distribution characteristics of a pMDI [16]. In this study, Ventolin<sup>®</sup> was used since it is one of the most commonly used medications in developing countries to treat respiratory problems in children and adults [17]. It mainly consists of salbutamol, the most frequently prescribed short-acting  $\beta$ -agonist (SABA) [18]. Thus, this paper

presented the optimization of the actuator nozzle inside the pMDI, which potentially increased the performance of pMDI to relieve respiratory problems.

## 2. Methodology

### 2.1 Geometrical Modelling

The geometrical modeling for the pMDI was created by using the actual scale of the commercial pMDI referred to in the previous literature [19]. The 3-Dimensional (3D) view of the pMDI and actuator nozzle was designed. Figure 1(a) showed the isometric view of pMDI. In contrast, the actuator nozzle in the pMDI is the hollow part of the nozzle (yellow color) presented in Figure 1(b). Figure 1(c) showed the internal components of the actuator nozzle.

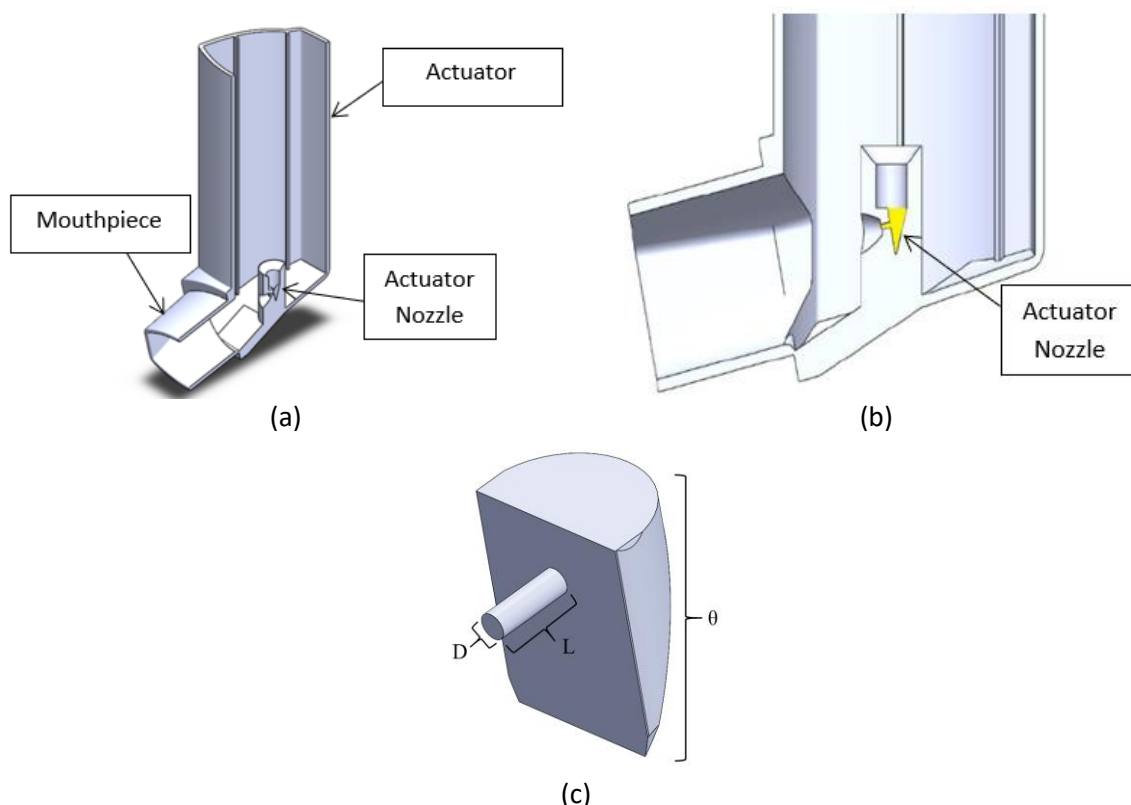


**Fig. 1.** Geometrical modeling of pMDI: (a) isometric view of pMDI inhaler, (b) the hollow part of the nozzle (yellow color), and (c) internal components of the actuator nozzle

Based on the simulation results performed by Oliveira *et al.*, [19] base design diameter could be determined for pMDI units; the diameter of the orifice was 0.49 mm, the actuator angle was  $165^\circ$ , and the length of the orifice was 1.50 mm. A parameter used to define the geometry of the actuator nozzle was orifice diameter (D), length of the orifice (L), and actuator angle ( $\theta$ ) that shown in Figure 1(c).

### 2.2 General Setup for Simulation

The setup used for the grid-independent test (GIT), meshing, and discrete phase model (DPM) in ANSYS Fluent version 19.2 and response surface methodology (RSM) were similar. The difference setup between this simulation is the 'Geometry' and 'Result' setup. In RSM, the 3D model was imported into the 'SpaceClaim Geometry', while in the ANSYS Fluent, the 3D model could be

imported into 'Geometry'. In the RSM 'Result', the 3D graphs could be produced and generating more than 30 design points for the actuator nozzle. In comparison, the 'Result' of ANSYS Fluent could generate particle tracking and spray plume of pMDI.

### 2.2.1 Grid independent test

The grid independent test (GIT) is necessary to preserve the model's precision. The precision was ensured by keeping the GIT value as low as possible, especially the skewness. Nevertheless, the coarse, medium and fine meshes were created in this GIT sequence. The solution could switch between the medium and fine meshes. GIT for the actuator nozzle is shown in Table 1. Nine (9) GITs were carried out. The best GIT value could be achieved with a low skewness mesh metric and a high orthogonal mesh metric. The table below showed that number three (3) was selected as it met the GIT criteria for further analysis.

**Table 1**  
 Grid independent test for commercial design A model

No	Number of nodes	Number of elements	Skewness mesh metric	Orthogonal mesh metric
1	346636	1573738	0.9455	0.9530
2	355176	1420206	0.9171	0.9143
3	314422	1570163	0.8560	0.9926
4	342386	1472759	0.9440	0.9544
5	301486	1463389	0.8639	0.9889
6	318616	1372876	0.9409	0.8891
7	315079	1364531	0.9417	0.8143
8	314246	1433875	0.9254	0.8456
9	335689	1448698	0.8896	0.9236

Table 2 listed the important properties of the drug formulations for propellant-HFA 134a, ethanol, and salbutamol.

**Table 2**  
 Property of drug formulation [20]

Properties	HFA-134a	Ethanol	Salbutamol
Density (kg/m <sup>3</sup> )	1311	790	1230
Specific heat (j/kg-k)	982	2470	-
Thermal conductivity (w/m-k)	0.0857	0.182	-
Viscosity (kg/m-s)	0.000211	0.0012	-
Molecular weight (kg/kmol)	102.032	46.07	337.387

### 2.2.2 Meshing

Figure 2 illustrated the meshed model in the mesh mode of component systems. An intelligent mesh tool was used in the current analysis to produce the most efficient and accurate mesh for the given geometry in a single click [21]. The compulsory measuring cell was completed with high efficiency and accuracy. The more elements there were, the more accurate the results. A larger number of elements, on the other hand, would result in a longer time taken to compute the results [22]. The solution's accuracy and stability had to be maintained to achieve a good mesh consistency. There was four mesh operating modes available in the simulation. The procedure began with determining the global mesh setup, followed by inserting a local mesh setting, generating the mesh,

and inspecting the mesh quality [23,24]. The curve object (cylinder) and the square object (box) could be selected as the convergent segment using proximity and curvature.

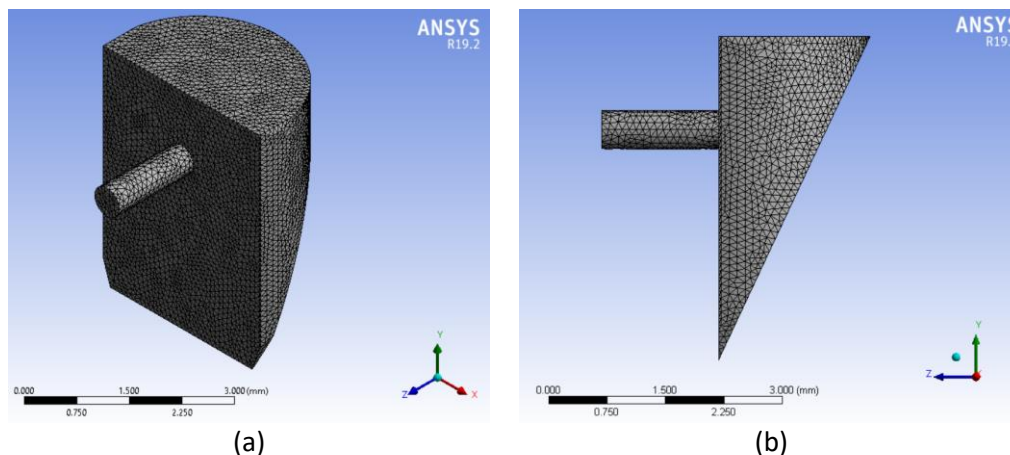


**Fig. 2.** Meshing process for internal parts in the actuator nozzle: (a) the meshing model of the nozzle (b) details views for the actuator angle in the actuator nozzle

### 2.2.3 Discrete phase model setup

This simulation aimed to show the configuration parameters best suited to the real-world case of an inhaler spray. In the discrete phase model, Rosin-Rammler was selected as a diameter distribution setup. The CFD solver accepted this type of distribution by inserting its parameters in Table 3 [20].

**Table 3**  
 Properties of Particle Diameter [20]

Parameter	Value
Diameter distribution	Rosin-Rammler
Minimum diameter ( $\mu\text{m}$ )	1.22
Maximum diameter ( $\mu\text{m}$ )	49.50
Mean diameter ( $\mu\text{m}$ )	16.54
Spread parameter	1.86

The amount of drug in one (1) puff ( $100\mu\text{g}$ ) was used and divided by the duration of a puff (0.1s). The flow rate of spray was calculated using the number of puffs and the duration of each puff. The solver spray configuration parameters were shown in Table 4.

**Table 4**  
 Properties of Spray Configuration

Parameter	Value
Spray type	Solid-cone [25,26]
Angle ( $^\circ$ )	10 [19]
Velocity (m/s)	100 [20]
Radius (m)	0.00025 [20,27]
Flow rate (kg/s)	$1e^{-6}$ [19]

The discrete phase model's parameters had already been tested in various configurations. Those listed here appeared to suit simulation purposes. The injection time step size (s) used for this DPM was particle time steps. As the limited period time (0.1s) was used for the injection, unsteady particle

tracking was selected. The spherical type used was the drag law, and this simulation activated the two-way coupling turbulence [20].

### 2.3 Mathematical Modelling in ANSYS Fluent 19.2

The  $k$ - $\varepsilon$  model is the most widely used for turbulence computations, with applications in various engineering domains. It is classified as a Reynolds-Averaged Navier–Stokes (RANS) based turbulence model, considering the eddy viscosity as linear; it is a two-equation model. This model accounts for the generation of turbulent kinetic energy ( $k$ ) as well as the turbulent dissipation of energy ( $\varepsilon$ ) [20]. The described model formulation is known as the Standard  $k$ - $\varepsilon$ , and it is calculated using Eq. (1) and Eq. (2).

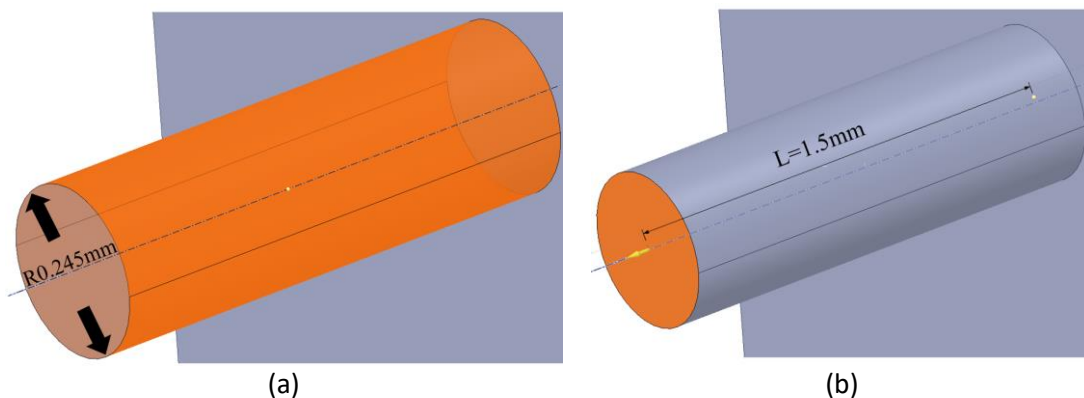
$$\frac{\partial}{\partial t}(\rho k) + \frac{\partial}{\partial x_i}(\rho k u_i) = \frac{\partial}{\partial x_j} \left[ \left( \mu + \frac{\mu_t}{\sigma_k} \right) \frac{\partial k}{\partial x_j} \right] + G_k - \rho \varepsilon \quad (1)$$

$$\frac{\partial}{\partial t}(\rho \varepsilon) + \frac{\partial}{\partial x_i}(\rho \varepsilon u_i) = \frac{\partial}{\partial x_j} \left[ \left( \mu + \frac{\mu_t}{\sigma_\varepsilon} \right) \frac{\partial \varepsilon}{\partial x_j} \right] + C_{1\varepsilon} \frac{\varepsilon}{k} G_k - C_{2\varepsilon} \rho \frac{\varepsilon^2}{k} \quad (2)$$

From the equation above,  $G_k$  define as the generation of turbulent kinetic energy due to the mean velocity gradients,  $\sigma_k$  and  $\sigma_\varepsilon$  are the turbulent Prandtl numbers for the  $k$  and  $\varepsilon$ , respectively.  $C_{1\varepsilon}$  and  $C_{2\varepsilon}$  are model constants [20].

#### 2.3.1 SpaceClaim in ANSYS version 19.2

The 3D drawing of internal parts of the actuator nozzle was imported to SpaceClaim in ANSYS. The base design diameter for pMDI units, including the diameter of the orifice, length of the orifice, and angle of the actuator, was set in the root part. In the root part, the diameter of the orifice was divided by two and become 0.245 mm because, in SpaceClaim, only the radius unit could be used. The root part diameter of the orifice is shown in Figure 3(a). Next, the orifice of 1.5 mm base design length was used, and for the base design angle of the actuator,  $360^\circ$  was set up in the root part. The root part of the length of the orifice and the angle of the actuator, as shown in Figure 3(b) and Figure 3(c), respectively.



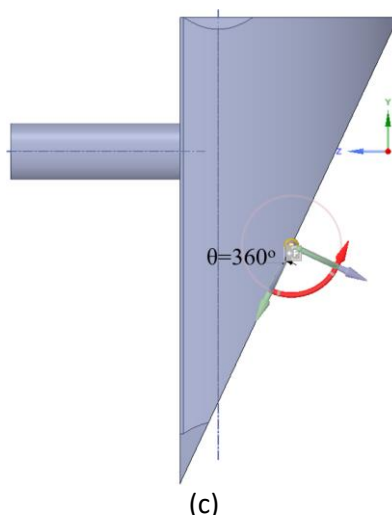


**Fig. 3.** The root part of the actuator nozzle: (a) diameter of the orifice, (b) length of the orifice, (c) actuator angle

### 2.3.2 Input parameter setup

The experiment was designed to define the input parameter that could affect the objective function of this research. Each input parameter of the actuator nozzle had to set the lower and upper bound design variables. In this case, the lower and upper boundary of the design variable was referred to from the previous literature review [28]. The range details of the input parameter and the design parameter are presented in Table 5.

**Table 5**  
 Input parameter for the design point in RSM [28]

No	Input parameter	Symbol notation	Lower bound	Upper bound
1	Diameter of orifice (mm)	P1	0.20	0.60
2	Length of orifice (mm)	P2	0.60	2.0
3	Actuator angle (°)	P3	352	360

### 2.4 Verification of Actuator Nozzle

In the verification system of actuator nozzle in pMDI, as shown in Table 5, four (4) parameters were chosen from the previous literature review: particle velocity magnitude, velocity magnitude, air temperature, and HFA mass. The model was verified according to Oliveira *et al.*, [19]. The relative error for geometric modeling was shown in Table 6. For the numerical simulation, the average limit for comparing two (2) simulated models must be below 10% [29]. As all variable parameters were below the limit and the geometric simulation was appropriate, further simulation could be performed.

**Table 6**  
 Verification of based model geometry

Velocity inlet (m/s)	Variable parameters	Result by Fluent 14.0 [20]	Result by Fluent 19.2	Relative error (%)
100	Particle velocity magnitude (m/s)	29.298	28.601	3.6
	Velocity magnitude (m/s)	10.29	10.91	6.0
	Air temperature (K)	293.15	293.01	0.05
	HFA mass fraction	0.0029	0.0027	6.2



## 2.5 Analysis of Particle Tracking

The three (3) potential designs were simulated, and the particle tracking was compared to the commercial design to analyze the performance of the potential new actuator nozzle design in pMDI. Then, the simulation analysis was performed at least three (3) times to obtain an average value. The injection number of drug particles, maximum particle velocity magnitude, and axial velocity were the first pieces of evidence to determine the best design among generated new designs for actuator nozzle. After a single puff was discharged, the injection particles and maximum particle velocity magnitude were recorded. Moreover, the maximum particles velocity magnitude was taken along the centerline of the spray cone at six axial locations (25 mm, 50 mm, 75 mm, 100 mm, 125 mm, and 150 mm) downstream from the edge of the pMDI mouthpiece, defined as the origin, after a single puff was discharged.

## 2.6 Spray Plume Analysis Setup

Three (3) tests were conducted to analyze the characteristic of the spray plume produced by actuator nozzle Design A, Design B, Design C, and Commercial pMDI, including the spray plume length, spray plume angle, and spray plume width. The ImageJ software was used to measure the spray plume length, angle, and width of potential new actuator nozzle designs in pMDI, including commercial devices. The spray plume length test was the first test that incorporated the potential new actuator nozzle design to validate their flow characteristic for relieving shortness of breath caused by COVID-19 and asthma. The spray plume length test was used to measure how far the drugs particle (HFA-134, salbutamol, and ethyl-alcohol liquid) traveled from the mouthpiece after 1 (one) puff before being inhaled to the targeted site. The second test was the spray plume angle. The spray plume angle test was conducted based on the plume's conical region extending from a vertex that occurs at or near the actuator tip, which traveled from the nozzle after 1 (one) puff. The analysis was furthered with spray plume width. The spray plume width test was measured at 30 mm from the mouthpiece after 1 (one) puff.

## 3. Results

### 3.1 Optimization of Inhaler Designs using Response Surface Method

Figure 4 shows the relationship of particle velocity magnitude between two (2) parameters; orifice's diameter and length of the actuator. The result was displayed in the RSM 3D graph. It could be seen that decreasing the diameter of the orifice could decrease the particle velocity magnitude. After a certain point, the particle velocity magnitude increased when the diameter further decreased. Furthermore, it was also shown that the particle velocity magnitude slightly increased and then steeply decreased when the orifice length decreased. Further decreasing in the length of the orifice gradually increased the particle velocity magnitude.



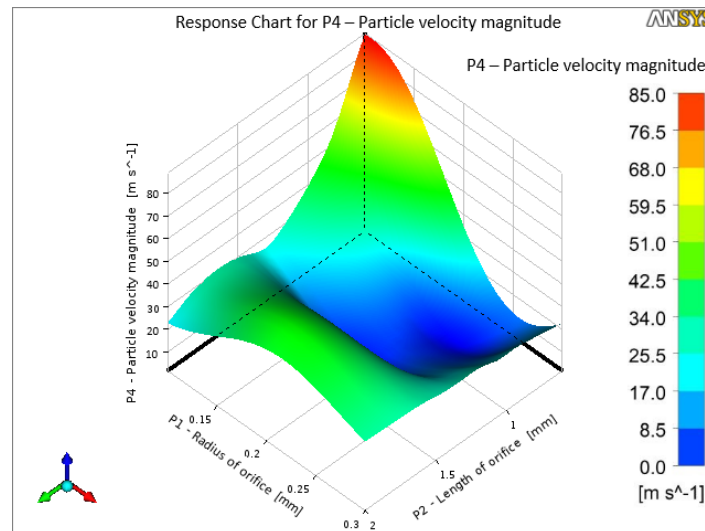


**Fig. 4.** Response surface chart on particle velocity magnitude against the diameter of orifice and length of the orifice

On the other hand, Figure 5 shows the relationship of particle velocity magnitude with the two (2) parameters; the orifice's diameter and the actuator's angle. The relationship between particle velocity magnitude and the orifice's diameter resulted in the same trend as in Figure 4, where decreasing the diameter of the orifice decreased the particle velocity magnitude. Further decrease in orifice diameter was gradually increased the particle velocity magnitude. Similarly, there had been a steady decrease in the particle velocity magnitude when the actuator angle was decreased. Further decrease in actuator angle was also increasing particle velocity magnitude.

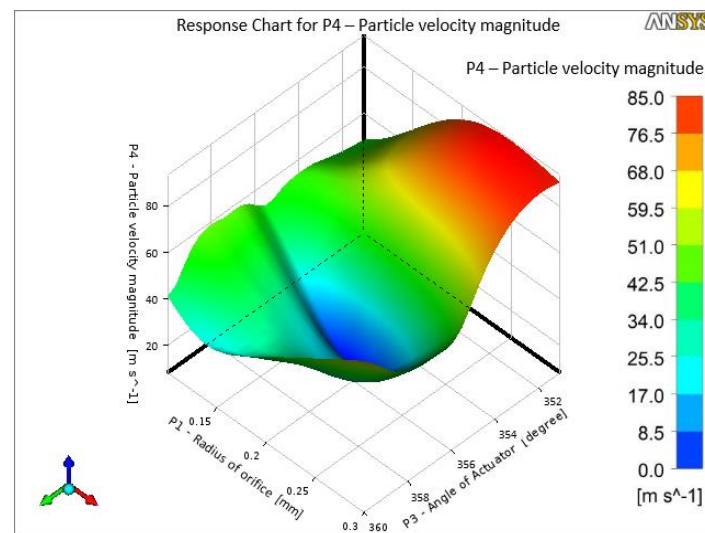


**Fig. 5.** Response surface chart on particle velocity magnitude against the diameter of orifice and actuator angle

These findings highlighted the complexities of interactions within the actuator design, which significantly impact particle velocity magnitude. Particle size is one of the well-known factors that affect drugs deposition in the lung [15]. Apart from particle size, one of the most critical aerosol features that influences inhaled medication deposition in the lungs is spray velocity magnitude [30]. According to Gabrio *et al.*, [31] the particle velocity magnitude can be decreased by utilizing a larger orifice diameter, which aligns with our result. Previously published reports have focused only on

orifice diameter as a primary factor used to modify the performance of typical pMDIs. In addition to spray plume characteristics, particle velocity magnitude can also be significantly influenced by actuator characteristics other than orifice diameter. Orifice length and actuator angle are two parameters of actuators that are not frequently examined or taken into account when evaluating pMDI performance. However, they have an impact on spray pattern formation in this research. The size of particles can also be affected by the orifice length, according to previous research [32]. However, the effect of orifice length on the spray velocity magnitude has not been widely explored. Similarly, actuator angle is also a feature of actuator that is not typically explored to improve the pMDI performance. However, Rahman *et al.*, [33] reported that the narrowest angle of the actuator produced the highest velocity magnitude, similar to our study.

According to RSM, optimizing the spray orifice diameter, length, and actuator angle could affect the particle velocity magnitude. Contributions to changes in particle velocity magnitude were significantly altered by changing orifice length and actuator angle, in addition to orifice diameter. It is crucial to optimize the design of the actuator because a higher particle velocity magnitude exceeding the acceptable range could cause turbulence, which reduced the respirable fraction of the particles [34]. The optimal velocity magnitude of particles further enhanced drug delivery to the lung [1]. Nevertheless, an unsuitable combination of actuator nozzle parameters could reduce fine particle mass (FPM) and increase throat deposition because the particles were too large to inhale [30]. Deposition of drugs particle (HFA-134, salbutamol, and ethyl-alcohol liquid) in the upper throat could cause medical conditions such as hoarseness and candidiasis. Meanwhile, increased alveolar deposition of much smaller particles could cause an increase in systemic adverse drug reactions resulting in increased toxicity [35]. This result suggested that optimizing the orifice diameter, length, and actuator angle could be vital for designing a good inhaler.

### 3.2 Selection of New Actuator Nozzle Base on The Design Point

The thirty (30) design points resulted from the combination of three (3) parameters; orifice diameter, length of the orifice, and actuator angle were generated in the RSM. Three (3) best design points (Design A, Design B, and Design C) were selected for further analysis to produce the new actuator nozzle (Table 7).

**Table 7**

Dimension of new optimum actuator nozzle of selected design point

Nozzle parameter	Design A	Design B	Design C
Diameter of orifice (mm)	0.20	0.30	0.40
Length of orifice (mm)	1.42	1.45	1.49
Actuator angle (°)	353	355	357

### 3.3 Analysis of Particle Tracking Using ANSYS Fluent Version 19.2

After RSM results were obtained, three (3) new actuator nozzle designs were simulated to see the qualitative image for the spray plume. The injection particle number, maximum particle velocity magnitude, and axial velocity were compared to the commercial pMDI.

#### 3.3.1 Injection particles number

Analysis of injection particles number was firstly employed to estimate the average particles injected from the actuator nozzle. The number of injection particles is vital in selecting the best design

as it could deliver more drugs into the lower respiratory, especially in the bronchiole and alveoli. According to Stein *et al.*, [16] the MDI actuator is a critical subsystem that significantly influences the delivery characteristics. The results showed that actuator nozzle Design C had the highest injection particle number compared to actuator nozzle Design A and Design B with 232457. The study also found that actuator nozzle Design C provided an excellent result for injection particles compared to commercial actuator nozzle pMDI (186845). The injection particle number of actuator nozzle Design C was increased by 24.41% compared with the commercial pMDI. Both actuator nozzle Design A and actuator nozzle Design B displayed a tremendously decreased number of particles injection, which is only around 76976 and 88127, respectively. Thus, actuator nozzle Design A and actuator nozzle Design B might not be suitable for producing a new actuator nozzle in pMDI. However, further analysis needed to be done to validate this result. The average injection particles for all actuator nozzle designs are shown in Figure 6.

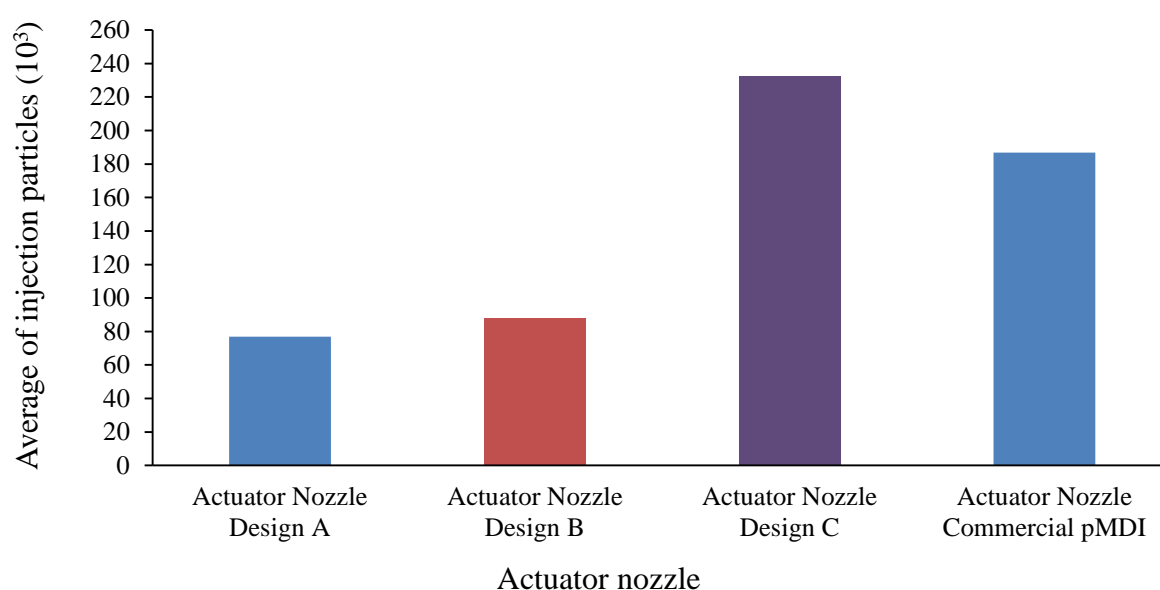


**Fig. 6.** Average injection particles for all actuator nozzle design

### 3.3.2 Particles velocity magnitude

The maximum particle velocity magnitude was further analyzed as the second factor to select the best new design for pMDI's actuator nozzle. According to Figure 7, it could be seen that those different combinations of nozzle parameters in the actuator nozzle produced different maximum particle velocity magnitude. Actuator nozzle Design A and Design B had the highest maximum particle velocity magnitude with 78.14 m/s and 56.32 m/s, respectively. Even though the actuator nozzle Design C (35.67 m/s) produced a slightly higher velocity than the commercial pMDI (28.6 m/s), its maximum particle velocity magnitude was still in the acceptable range, ranging from 26.94 - 43.20 m/s [33]. As mentioned before, it is crucial to get the optimal maximum particle velocity magnitude as higher velocity could cause turbulence, which could reduce the respirable fraction of the particles [36]. According to Miller [37] higher maximum particle velocity magnitude increased particle deposition in the pharynx, decreasing deposition in the lower respiratory. The initial high velocity in conjunction with the larger particle sizes resulted in a sizeable proportion of particles impacting the mouth and throat before the propellant evaporates, decreasing the number of particles available for inhalation [38]. This result could be seen in both actuator nozzle Design A and Design B, which had the highest maximum particle velocity magnitude exceeding the acceptable range. This result

supported the previous analysis in which the interactions within the actuator parameters of Design A and Design B might not be suitable for producing a new actuator nozzle in pMDI as their maximum particle velocity magnitude was out of acceptable range.

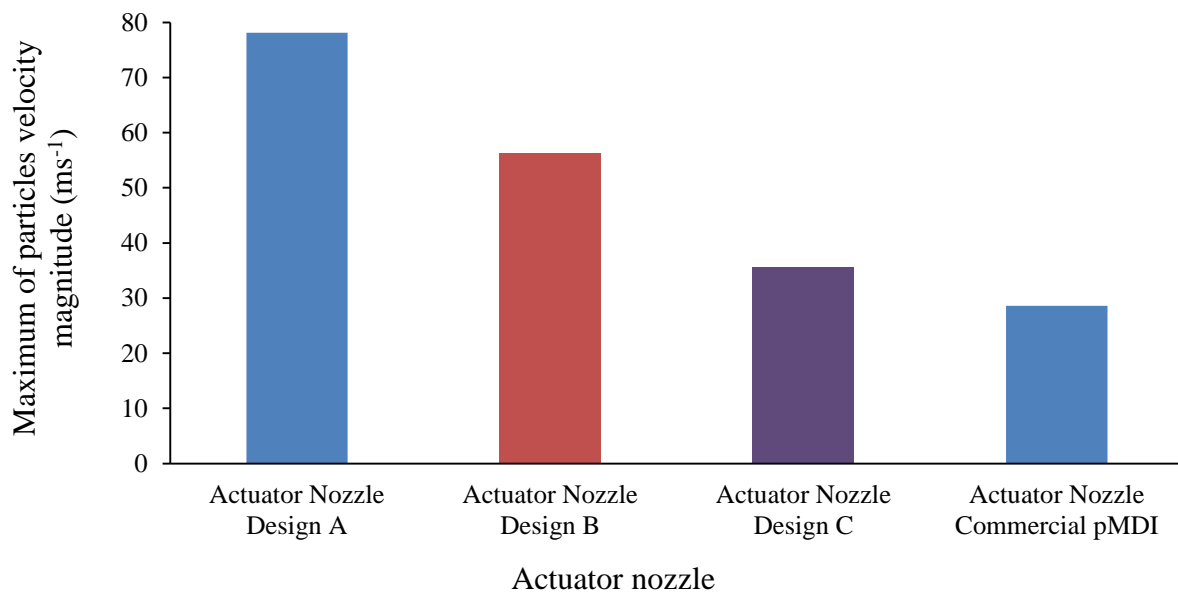


**Fig. 7.** Average of maximum particles velocity magnitude for all actuator nozzle design

### 3.3.3 Relationship between maximum particles velocity magnitude and axial distance

A similar axial distance trend was observed in all three (3) potential actuator nozzle (Design A, Design B, and Design C) and actuator nozzle Commercial pMDI. The droplets' maximum velocity magnitude decreased along with the axial distance due to the momentum exchange with the air velocity. The particles located downstream of the actuator mouthpiece rapidly decelerate until they match the air velocity (0.03-0.04 m/s). In line with the previous study, the maximum velocity magnitude droplets decreased along the axial length from the nozzle due to the dynamic exchange [20]. Oliveira *et al.*, [20] demonstrated that the plume behaved like a spray up to a distance of 75 mm from the nozzle. When an aerosol downstream the distance, gas was influencing the droplet motion until it reached air velocity. Figure 8 shows the maximum particle velocity magnitude with axial distance for all actuator nozzle designs.

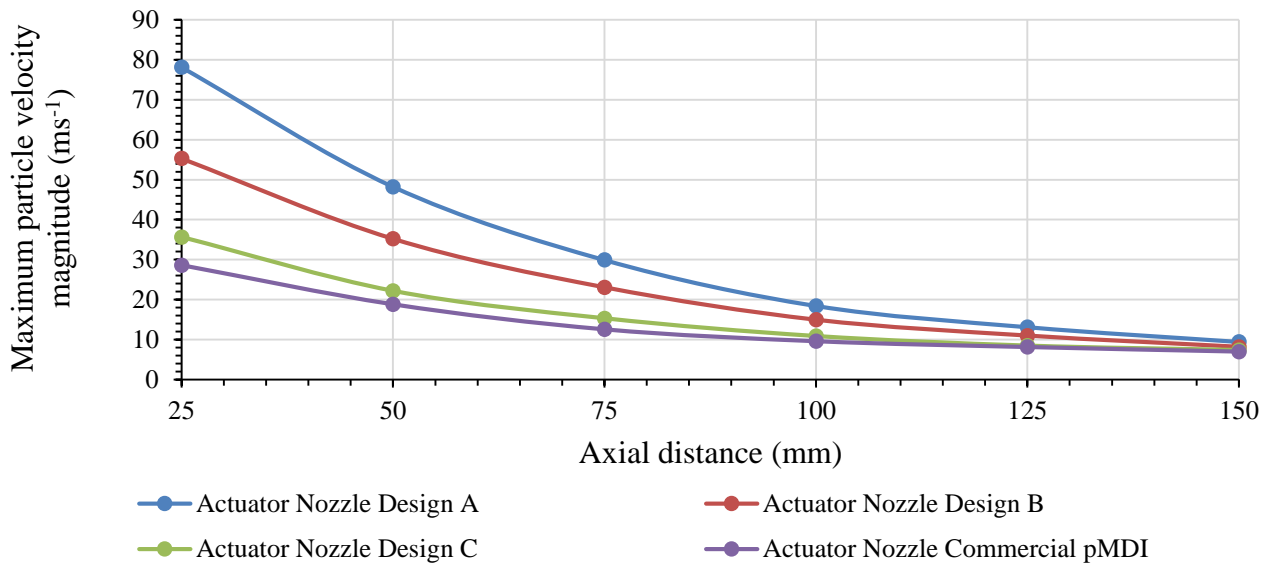
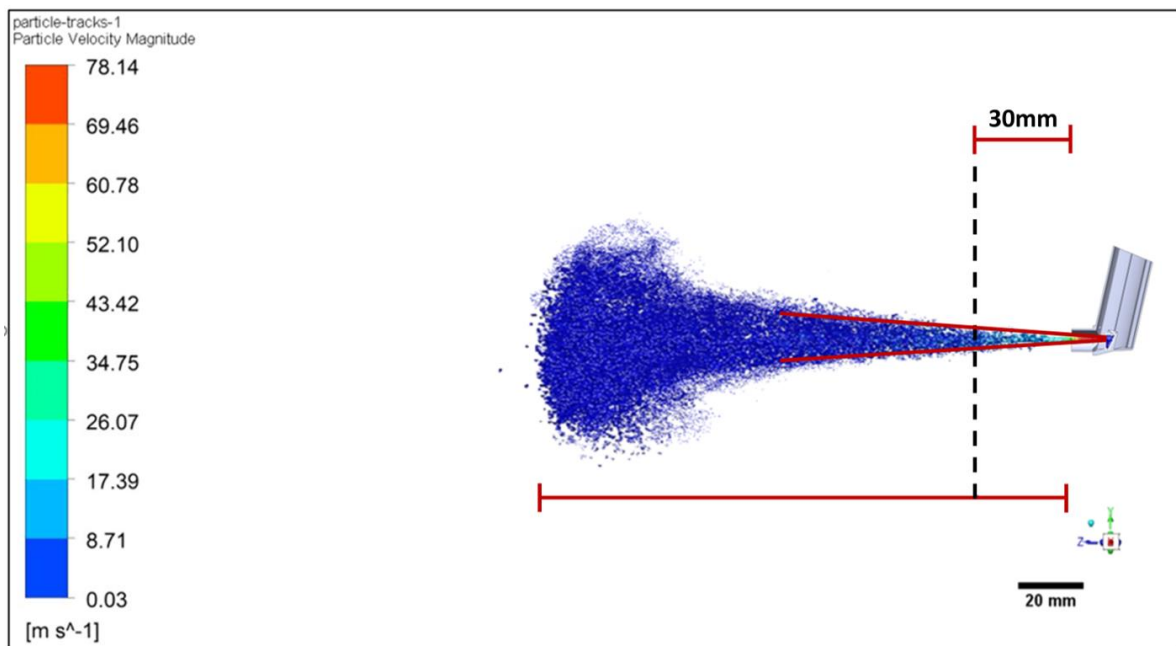


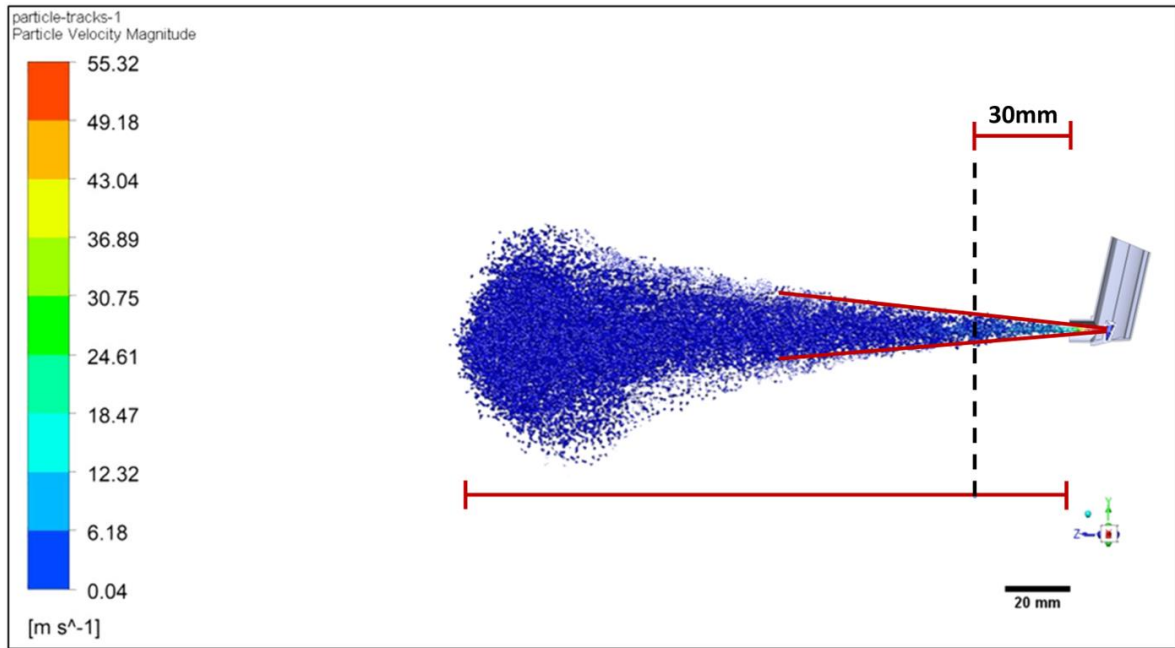
**Fig. 8.** Maximum particles velocity magnitude with axial distance for all actuator nozzle design

### 3.4 Spray Plume Analysis for All Actuator Nozzle Design

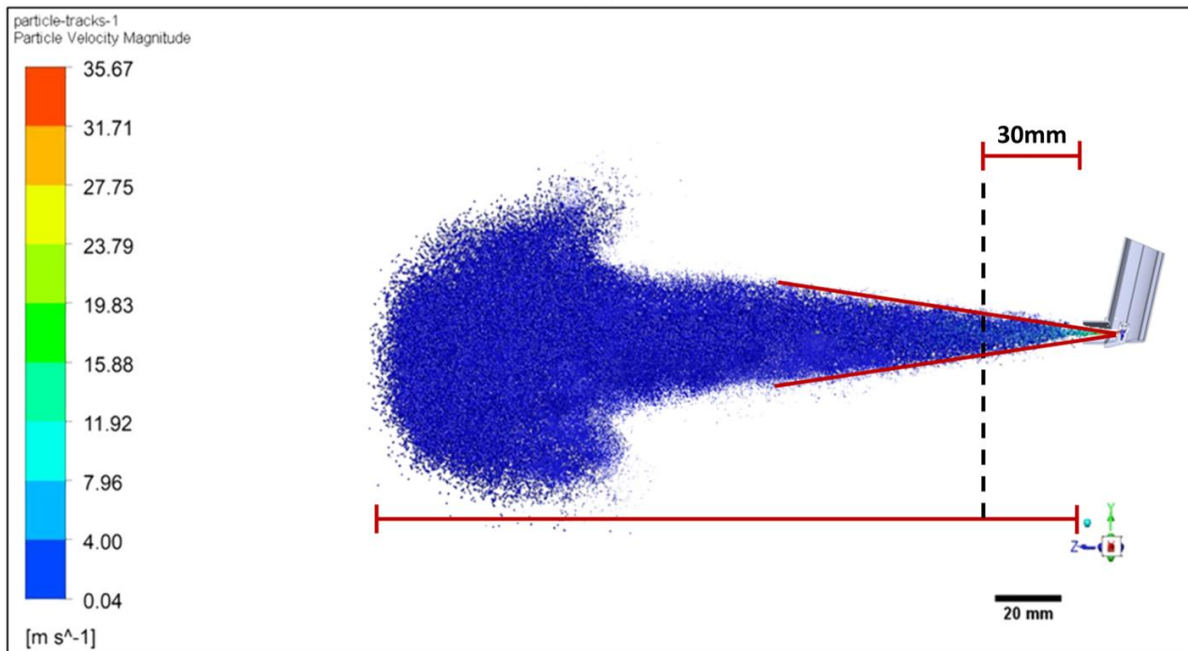
In this study, the discrete phase model (DPM) in ANSYS Fluent version 19.2 was used to find the spray plume for the actuator nozzle Design A, Design B, Design C, and Commercial pMDI. As mentioned above, the spray length was measured from the edge of the pMDI mouthpiece, defined as the origin. The spray plume angle was conducted based on the plume’s conical region extending from a vertex that occurs at or near the actuator tip. Lastly, the plume width was measured at 30 mm from the mouthpiece after 1 (one) puff. Figure 9 showed the simulation result for the spray plume for all actuator nozzle designs.



(a)

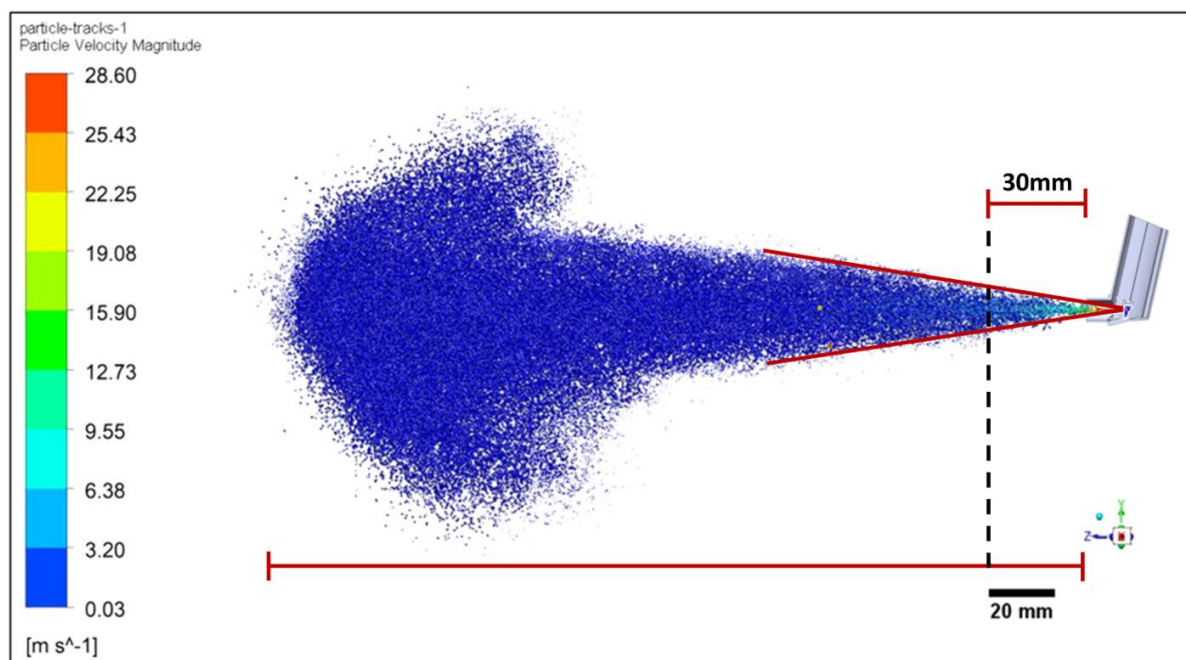


(b)



(c)





(d)

**Fig. 9.** Simulation result for the spray plume for all actuator nozzle designs: (a) actuator nozzle Design A, (b) actuator nozzle Design B, (c) actuator nozzle Design C, (d) actuator nozzle Commercial pMDI

The orifice diameter, length, and actuator angle had been proven to affect spray patterns [33,39]. According to Figure 9, the spray plume length increased linearly with the decreasing of particle velocity magnitude. This finding suggested that a higher particle velocity magnitude produced a smaller spray length. The reason is that higher injection pressure resulted in a higher resultant axial velocity component, increasing the spray plume tendency to disintegrate earlier [40]. It had also been observed that the spray plume angle increased with the decrease of particle velocity magnitude. This view is supported by Chu *et al.*, [41] where the lower velocity magnitude will increase the spray cone angle and produces the longest breakup length. In addition, it is clear that when the particle velocity magnitude decreased, the spray plume width was also increased. Maniarasan and Nicholas [42] validated this statement by demonstrating that the nozzle with the lowest particle velocity magnitude produced the widest spray plume. Table 8 shows the summary of the spray plume result regarding length, angle, and width for all actuator nozzle designs.

**Table 8**

Spray plume result for all actuator nozzle design

Actuator nozzle	Particle velocity magnitude (m/s)	Spray plume		
		Length (mm)	Angle (°)	Width (mm)
Design A	78.14	162.94	9.69	7.24
Design B	55.32	187.74	12.17	9.86
Design C	35.67	210.619	14.754	11.537
Commercial pMDI	28.60	238.783	16.231	12.987

#### 4. Conclusions

In summary, it had been shown that the diameter of the orifice, length of the orifice, and actuator angle could affect the spray development for pMDI. Important observations were made concerning the importance of previously unstudied actuator design parameters. Using the response surface methodology (RSM), three (3) new actuator nozzle designs for pMDI were analyzed; among them,



actuator nozzle Design C was highly recommended to produce a new actuator nozzle design for pMDI. Combining the nozzle parameters for the actuator nozzle, such as the orifice diameter, length of the orifice, and actuator angle, was essential to improve drug particles' deposition in the lower respiratory by decreasing the particle velocity magnitude and the particles size. Based on these computational results and considering the analysis of particle tracking and analysis of spray plume in the device, specific improvements to the pMDI design became apparent. The finding of this study could be helpful as a reference for producing a new actuator nozzle design to relieve respiratory problems by decreasing the number of experiments and trials. However, a detailed study is necessary to validate the drug deposition in the lung using a modified design. The rational design of pMDIs should consider these variables and formulation techniques and change the actuator nozzle's geometry.

### Acknowledgment

The authors would like to thank the Ministry of Higher Education Malaysia for supporting this research under Fundamental Research Grant Scheme Vot No. FRGS/1/2018/TK03/UTHM/03/5. The authors would also like to thank the Centre for Graduate Studies UTHM for partly funding this paper.

### References

- [1] Zhou, Qi Tony, Patricia Tang, Sharon Shui Yee Leung, John Gar Yan Chan, and Hak-Kim Chan. "Emerging inhalation aerosol devices and strategies: where are we headed?." *Advanced Drug Delivery Reviews* 75 (2014): 3-17. <https://doi.org/10.1016/j.addr.2014.03.006>
- [2] Oort, Michiel Van. "In vitro testing of dry powder inhalers." *Aerosol Science and Technology* 22, no. 4 (1995): 364-373. <https://doi.org/10.1080/02786829408959754>
- [3] Geller, David E. "Comparing clinical features of the nebulizer, metered-dose inhaler, and dry powder inhaler." *Respiratory Care* 50, no. 10 (2005): 1313-1322.
- [4] Kaialy, Waseem, Martyn Ticehurst, and Ali Nokhodchi. "Dry powder inhalers: mechanistic evaluation of lactose formulations containing salbutamol sulphate." *International Journal of Pharmaceutics* 423, no. 2 (2012): 184-194. <https://doi.org/10.1016/j.ijpharm.2011.12.018>
- [5] Young, Paul M., Doreen Roberts, Herbert Chiou, William Rae, Hak-Kim Chan, and Daniela Traini. "Composite carriers improve the aerosolisation efficiency of drugs for respiratory delivery." *Journal of Aerosol Science* 39, no. 1 (2008): 82-93. <https://doi.org/10.1016/j.jaerosci.2007.10.003>
- [6] Yazdani, A., M. Normandie, Morteza Yousefi, M. S. Saidi, and Goodarz Ahmadi. "Transport and deposition of pharmaceutical particles in three commercial spacer-MDI combinations." *Computers in Biology and Medicine* 54 (2014): 145-155. <https://doi.org/10.1016/j.compbiomed.2014.08.001>
- [7] Stein, Stephen W., and Charles G. Thiel. "The history of therapeutic aerosols: a chronological review." *Journal of Aerosol Medicine and Pulmonary Drug Delivery* 30, no. 1 (2017): 20-41. <https://doi.org/10.1089/jamp.2016.1297>
- [8] Leach, Chet L., Patricia J. Davidson, Bruce E. Hasselquist, and Robert J. Boudreau. "Influence of particle size and patient dosing technique on lung deposition of HFA-beclomethasone from a metered dose inhaler." *Journal of Aerosol Medicine* 18, no. 4 (2005): 379-385. <https://doi.org/10.1089/jam.2005.18.379>
- [9] Dolovich, Myrna. "New delivery systems and propellants." *Canadian Respiratory Journal* 6, no. 3 (1999): 290-295. <https://doi.org/10.1155/1999/682405>
- [10] Ross, Danna L., and Brian J. Gabrio. "Advances in metered dose inhaler technology with the development of a chlorofluorocarbon-free drug delivery system." *Journal of Aerosol Medicine* 12, no. 3 (1999): 151-160. <https://doi.org/10.1089/jam.1999.12.151>
- [11] Usmani, Omar S. "Choosing the right inhaler for your asthma or COPD patient." *Therapeutics and Clinical Risk Management* 15 (2019): 461-472. <https://doi.org/10.2147/TCRM.S160365>
- [12] Sharma, Atul, Swapnil Tiwari, Manas Kanti Deb, and Jean Louis Marty. "Severe acute respiratory syndrome coronavirus-2 (SARS-CoV-2): a global pandemic and treatment strategies." *International Journal of Antimicrobial Agents* 56, no. 2 (2020): 106054. <https://doi.org/10.1016/j.ijantimicag.2020.106054>
- [13] Milenkovic, Jovana, Aleck H. Alexopoulos, and Costas Kiparissides. "Optimization of a DPI inhaler: a computational approach." *Journal of Pharmaceutical Sciences* 106, no. 3 (2017): 850-858. <https://doi.org/10.1016/j.xphs.2016.11.008>

- [14] Sommerfeld, Martin, and Silvio Schmalfuß. "Numerical analysis of carrier particle motion in a dry powder inhaler." *Journal of Fluids Engineering* 138, no. 4 (2016): 041308. <https://doi.org/10.1115/1.4031693>
- [15] Smyth, Hugh, Geoff Brace, Tony Barbour, Jim Gallion, Joe Grove, and Anthony J. Hickey. "Spray pattern analysis for metered dose inhalers: effect of actuator design." *Pharmaceutical Research* 23, no. 7 (2006): 1591-1596. <https://doi.org/10.1007/s11095-006-0280-z>
- [16] Stein, Stephen W., Poonam Sheth, P. David Hodson, and Paul B. Myrdal. "Advances in metered dose inhaler technology: hardware development." *AAPS PharmSciTech* 15, no. 2 (2014): 326-338. <https://doi.org/10.1208/s12249-013-0062-y>
- [17] Crompton, Graham. "A brief history of inhaled asthma therapy over the last fifty years." *Primary Care Respiratory Journal* 15, no. 6 (2006): 326-331. <https://doi.org/10.1016/j.pcrj.2006.09.002>
- [18] Zuidgeest, Mira G., Henriëtte A. Smit, Madelon Bracke, Alet H. Wijga, Bert Brunekreef, Maarten O. Hoekstra, Jorrit Gerritsen et al. "Persistence of asthma medication use in preschool children." *Respiratory Medicine* 102, no. 10 (2008): 1446-1451. <https://doi.org/10.1016/j.rmed.2008.04.003>
- [19] Oliveira, Ricardo F., Ana C. Ferreira, Senhorinha F. Teixeira, José C. Teixeira, and Helena C. Marques. "pMDI spray plume analysis: a CFD study." In *Proceedings of the World Congress on Engineering*, vol. 3. 2013.
- [20] Oliveira, Ricardo F., S. F. C. F. Teixeira, José C. Teixeira, Luís F. Silva, and Henedina Antunes. "pMDI sprays: Theory, experiment and numerical simulation." *Advances in Modeling of Fluid Dynamics* 300 (2012): 254-292.
- [21] Uppu, Shiva Prasad, Dindigala Manisha, Gudey Dharani Devi, Pranav Chengalwa, and Boppana Vaishnavi Devi. "Aerodynamic analysis of a dragonfly." *Journal of Advanced Research in Fluid Mechanics and Thermal Sciences* 51, no. 1 (2018): 31-41.
- [22] Dahalan, Md Nizam, Ahmad Fitri Suni, Iskandar Shah Ishak, Nik Ahmad Ridhwan Nik Mohd, and Shabudin Mat. "Aerodynamic study of air flow over a curved fin rocket." *Journal of Advanced Research in Fluid Mechanics and Thermal Sciences* 40, no. 1 (2017): 46-58.
- [23] Mat, Mohamad Nur Hidayat, and Norzelawati Asmuin. "Optimizing nozzle geometry of dry ice blasting using CFD for the reduction of noise emission." *International Journal of Integrated Engineering* 10, no. 5 (2018): 130-135. <https://doi.org/10.30880/ijie.2018.10.05.019>
- [24] Mat, Mohamad Nur Hidayat, Nor Zelawati Asmuin, Md Faisal Md Basir, Marjan Goodarzi, Muhammad Faqhrurrazi Abd Rahman, Riyadhthusollehan Khairulfuaad, Balasem Abdulameer Jabbar, and Mohd Shareduwan Mohd Kasihmuddin. "Influence of divergent length on the gas-particle flow in dual hose dry ice blasting nozzle geometry." *Powder Technology* 364 (2020): 152-158. <https://doi.org/10.1016/j.powtec.2020.01.060>
- [25] Chen, Yang, Paul M. Young, David F. Fletcher, Hak Kim Chan, Edward Long, David Lewis, Tanya Church, and Daniela Traini. "The influence of actuator materials and nozzle designs on electrostatic charge of pressurized metered dose inhaler (pMDI) formulations." *Pharmaceutical Research* 31, no. 5 (2014): 1325-1337. <https://doi.org/10.1007/s11095-013-1253-7>
- [26] Cheng, Y. S., C. S. Fu, D. Yazzie, and Y. Zhou. "Respiratory deposition patterns of salbutamol pMDI with CFC and HFA-134a formulations in a human airway replica." *Journal of Aerosol Medicine* 14, no. 2 (2001): 255-266. <https://doi.org/10.1089/08942680152484180>
- [27] Clark, Andrew R. "MDIs: physics of aerosol formation." *Journal of Aerosol Medicine* 9, no. s1 (1996): S19-26. <https://doi.org/10.1089/jam.1996.9.Suppl.1.S-19>
- [28] Lewis, David. "Metered-dose inhalers: actuators old and new." *Expert Opinion on Drug Delivery* 4, no. 3 (2007): 235-245. <https://doi.org/10.1517/17425247.4.3.235>
- [29] Goswami, Mayank, Sanjeev Kumar, and Prabhat Munshi. "Correlation between numerical simulation and limited data experimental technique for estimation of nitrogen flowing in LMMHD loop." *Flow Measurement and Instrumentation* 46 (2015): 80-86. <https://doi.org/10.1016/j.flowmeasinst.2015.10.002>
- [30] Hochrainer, Dieter, Hubert Hölz, Christoph Kreher, Luigi Scaffidi, Michael Spallek, and Herbert Wachtel. "Comparison of the aerosol velocity and spray duration of Respimat® Soft Mist™ inhaler and pressurized metered dose inhalers." *Journal of Aerosol Medicine* 18, no. 3 (2005): 273-282. <https://doi.org/10.1089/jam.2005.18.273>
- [31] Gabrio, Brian J., Stephen W. Stein, and David J. Velasquez. "A new method to evaluate plume characteristics of hydrofluoroalkane and chlorofluorocarbon metered dose inhalers." *International Journal of Pharmaceutics* 186, no. 1 (1999): 3-12. [https://doi.org/10.1016/S0378-5173\(99\)00133-7](https://doi.org/10.1016/S0378-5173(99)00133-7)
- [32] Zhu, Bing, Daniela Traini, and Paul Young. "Aerosol particle generation from solution-based pressurized metered dose inhalers: a technical overview of parameters that influence respiratory deposition." *Pharmaceutical Development and Technology* 20, no. 8 (2015): 897-910. <https://doi.org/10.3109/10837450.2014.959176>
- [33] Rahman, Muhammad Faqhrurrazi Abd, Nor Zelawati Asmuin, Ishkrizat Taib, Mohamad Nur Hidayat Mat, and Riyadhthusollehan Khairulfuaad. "Influence of Actuator Nozzle Angle on the Flow Characteristics in Pressurized-Metered Dose Inhaler Using CFD." *CFD Letters* 12, no. 6 (2020): 67-79. <https://doi.org/10.37934/cfdl.12.6.6779>

- [34] Berry, Julianne, Susan Heimbecher, John L. Hart, and Joel Sequeira. "Influence of the metering chamber volume and actuator design on the aerodynamic particle size of a metered dose inhaler." *Drug Development and Industrial Pharmacy* 29, no. 8 (2003): 865-876. <https://doi.org/10.1081/DDC-120024182>
- [35] Gumani, D., William Newmarch, Angelica Puopolo, and Brian Casserly. "Inhaler technology." *International Journal of Respiratory and Pulmonary Medicine* 3 (2016): 064.
- [36] Alatrash, Abubaker, and Edgar Matida. "Characterization of medication velocity and size distribution from pressurized metered-dose inhalers by phase Doppler anemometry." *Journal of Aerosol Medicine and Pulmonary Drug Delivery* 29, no. 6 (2016): 501-513. <https://doi.org/10.1089/jamp.2015.1264>
- [37] Miller, Carrie J. "Inhaled Medications." In *Small Animal Critical Care Medicine*, pp. 903-906. WB Saunders, 2015. <https://doi.org/10.1016/B978-1-4557-0306-7.00172-0>
- [38] Fonceca, Angela Mary, William Graham Fox Ditcham, Mark L. Everard, and Sunalene Devadason. "Drug administration by inhalation in children." *Kendig's Disorders of the Respiratory Tract in Children* (2019): 257-271. <https://doi.org/10.1016/B978-0-323-44887-1.00016-X>
- [39] Smyth, Hugh, Geoff Brace, Tony Barbour, Jim Gallion, Joe Grove, and Anthony J. Hickey. "Spray pattern analysis for metered dose inhalers: effect of actuator design." *Pharmaceutical Research* 23, no. 7 (2006): 1591-1596. <https://doi.org/10.1007/s11095-006-0280-z>
- [40] Hussein, A., M. Hafiz, W. Wisnoe, and M. Jasmi. "Effect of orifice diameter on characteristics of hollow cone swirl spray emanating from simplex nozzles." In *AIP Conference Proceedings*, vol. 1440, no. 1, pp. 124-129. American Institute of Physics, 2012. <https://doi.org/10.1063/1.4704210>
- [41] Chu, Chia-Chien, Shyan-Fu Chou, Heng-I. Lin, and Yi-Hai Liann. "An experimental investigation of swirl atomizer sprays." *Heat and Mass Transfer* 45, no. 1 (2008): 11-22. <https://doi.org/10.1007/s00231-008-0389-1>
- [42] Maniarasan, P., and M. T. Nicholas. "Performance prediction and experimental investigation of swirl atomizer for evaporation of water at low pressure." *International Journal of Applied Engineering Research* 1, no. 3 (2006): 353-364.